Published in final edited form as:

Cancer Res. 2012 February 15; 72(4): 958–968. doi:10.1158/0008-5472.CAN-11-0042.

A Positive Feedback Signaling Loop between ATM and the Vitamin D Receptor Is Critical for Cancer Chemoprevention by Vitamin D

Huei-Ju Ting[1,2], **Sayeda Yasmin-Karim**[3], **Shian-Jang Yan**[6], **Jong-Wei Hsu**[2], **Tzu-Hua Lin**[2], **Weisi Zeng**[1], **James Messing**[1], **Tzong-Jeng Sheu**[4], **Bo-Ying Bao**[5], **Willis X. Li**[6], **Edward Messing**[1,2], and **Yi-Fen Lee**[1,2]

[1]Department of Urology, University of Rochester, Rochester, New York

[2]Department of Pathology and Laboratory Medicine, University of Rochester, Rochester, New York

[3]Department of Chemical Engineering, University of Rochester, Rochester, New York

[4]Department of Orthopedics, University of Rochester, Rochester, New York

[5]School of Pharmacy, China Medical University, Taichung, Taiwan

[6]Department of Medicine, University of California, San Diego, California

Abstract

Both epidemiologic and laboratory studies have shown the chemopreventive effects of 1α,25-dihydroxyvitamin D_3 (1,25-VD) in tumorigenesis. However, understanding of the molecular mechanism by which 1,25-VD prevents tumorigenesis remains incomplete. In this study, we used an established mouse model of chemical carcinogenesis to investigate how 1,25-VD prevents malignant transformation. In this model, 1,25-VD promoted expression of the DNA repair genes *RAD50* and *ATM,* both of which are critical for mediating the signaling responses to DNA damage. Correspondingly, 1,25-VD protected cells from genotoxic stress and growth inhibition by promoting double-strand break DNA repair. Depletion of the vitamin D receptor (VDR) reduced these genoprotective effects and drove malignant transformation that could not be prevented by 1,25-VD, defining an essential role for VDR in mediating the anticancer effects of 1,25-VD. Notably, genotoxic stress activated ATM and VDR through phosphorylation of VDR. Mutations in VDR at putative ATM phosphorylation sites impaired the ability of ATM to enhance VDR transactivation activity, diminishing 1,25-VD-mediated induction of ATM and RAD50 expression. Together, our findings identify a novel vitamin D-mediated chemopreventive mechanism involving a positive feedback loop between the DNA repair proteins ATM and VDR.

Corresponding Author: Yi-Fen Lee, Department of Urology, University of Rochester Medical Center, 601 Elmwood Avenue, Box 656, Rochester, NY 14642. Phone: 585-275-9702; yifen_lee@urmc.rochester.edu.

Disclosure of Potential Conflicts of Interest

No potential conflicts of interests were disclosed.

The costs of publication of this article were defrayed in part by the payment of page charges. This article must therefore be hereby marked *advertisement* in accordance with 18 U.S.C. Section 1734 solely to indicate this fact.

Note: Supplementary data for this article are available at Cancer Research Online (http://cancerres.aacrjournals.org/).

Introduction

The chemopreventive role of vitamin D in numerous types of cancer, including colorectal, breast, and prostate cancer was first suggested by epidemiologic studies (1–3). Further studies showed that vitamin D deficiency is associated with risk of cancer development (4–6). Preclinical studies support the chemopreventive effect of vitamin D in carcinogen-induced animal tumor models (7–9). Moreover, vitamin D receptor (VDR)-deficient mice exhibit higher carcinogen-induced tumor incidence in numerous tissues (10). Therefore, vitamin D supplementation and the activation of the VDR signaling pathway protect organisms from malignant transformation.

Cells are constantly challenged by spontaneous errors as well as environmental insults that lead to DNA damage. Accumulated genomic mutations from improperly repaired DNA damages can lead to malignant transformation. Several studies indicate that vitamin D attenuates DNA damage levels. Vitamin D can reduce ultraviolet light irradiation-induced DNA photoproducts and chromosome aberrations in diethylnitrosamine-treated liver (11–13). This could result from decreasing sources of genotoxic stress, for example, the anti-oxidant effect of vitamin D protects cells against oxidative insults (13–16). Recently, accumulated evidence from gene profiling shows that vitamin D induces the expression of DNA repair genes (17, 18), suggesting that vitamin D could facilitate DNA repair pathways.

DNA double-strand breaks (DSB), mostly caused by exposure to reactive oxygen species (ROS), ionizing radiation (IR), or generated during replication of single-strand breaks, are susceptible to exonucleases that lead to loss of large genomic regions. Once DSBs occur, formation of the Mre11/Rad50/NBS complex recruits the DNA damage response (DDR) signaling kinase, ATM (ataxia telangiectasia mutated), to the DSB and then the H2A histone family member X (H2Ax) is phosphorylated by ATM. The formation of foci containing serine 139-phosphorylated H2Ax (γ-H2Ax) is required for retaining mediator proteins, TP53BP1, MDC1, BRCA1, and the Mre11/Rad50/NBS complex at the DSB. These mediator proteins facilitate assembly of the DNA repair machinery to conduct the repair of DSB (19). There are 2 DSB repair pathways, homologous recombination (HR) and non-homologous end joining (NHEJ). HR uses Holliday junction formation to facilitate strand transfer exchange between sister chromatids and is therefore less error prone. NHEJ is an efficient but more error-prone repair pathway (20). Malfunctioned DDR signaling proteins and repair machineries can have catastrophic consequences that lead to premature aging and tumorigenesis (21, 22). Recent findings discovered that the DDR signaling cascades ATM/Chk2/p53 pathway is upregulated by oncogenic stress, and inhibition of ATM leads to large and invasive tumor development (23, 24). These studies conclude that the ATM signaling pathway is an anticancer barrier of early-stage tumorigenesis.

In the current study, we show a cross-talk between DDR and vitamin D signaling in protecting DNA from genotoxic insults which is one mechanism mediating the chemopreventive effect of vitamin D against tumorigenesis.

Materials and Methods

Plasmids and reagents

NHEJ reporter, GFP-Pem1-Ad2, was a generous gift from Dr. Vera Gorbunova (University of Rochester, Rochester, NY). pDsRed-N1 was purchased from Clontech. Plasmids for GFP-based homologous recombination assay system, pDR-GFP and pCβASce, were generous gifts from Dr. Maria Jasin (Memorial Sloan-Kettering Cancer Center, New York). The plasmids pGEX-KG-VDR-L, pGEX-KG-VDR-L1, and pGEX-KG-VDR-L2 were constructed by PCR amplifying VDR fragments with oligomers containing Bam*HI* and Xba*I* sites, which were then inserted into pGEX-KG vectors (Promega). pcDNA3-flag-ATM and pcDNA-flag-ATMkd were generous gifts from Dr. Michael Kastan (St. Jude Children's Research Hospital, Memphis, TN). pcDNA-flag-VDR was constructed by PCR amplifying VDR cDNA using oligomers containing *Bam*HI and *Xba*I sites and then inserted into pcDNA-flag plasmids. pcDNA-flag-mutant VDRs were constructed by QuikChange Site-Directed Mutagenesis kit (Stratagene). Antibodies of γ-H2Ax (clone JBW301) and phospho-ATM (serine 1981) were purchased from Millipore; H2Ax was from Bethyl Lab; VDR (H-81), ATM, and β-actin were from Santa Cruz; phosphoserine was from Zymed. ATM-specific inhibitor, KU55933, was purchased from Selkeck. Mouse embryonic fibroblast (MEF) cells from $VDR^{-/+}$ and $VDR^{-/-}$ mice were generous gifts from Dr. Jun Sun (University of Rochester Medical Center). RWPE-1 is from American Type Culture Collection.

Anchorage-independent colony-forming assay

BPH-1 cells were maintained in 10% FBS supplemented RPMI medium. MEFs derived from $VDR^{-/+}$ and $VDR^{-/-}$ mice were maintained in 10% FBS-supplemented Dulbecco's Modified Eagle's Medium. Cells suspended at a density of 1×10^5 cells/mL in 0.4% Noble agar (Sigma) containing medium were seeded on top of underlayer of 0.8% agarose-containing medium in culture plates. Media were refreshed twice per week for 3 weeks. Colonies were stained with *p*-iodonitrotetrazolium violet (Sigma), photographed, and counted.

Xenograft mouse tumor model

The study was approved by the University of Rochester Committee on Animal Resources, and the mice were kept in a specific pathogen-free environment at the animal facility of the University of Rochester Medical Center. Young adult male athymic NCr-*nu/nu* mice (NCI-Frederick, Frederick, MD) at 8 to 10 weeks of age were subcutaneously injected with *N*-nitroso-*N*-methylurea (NMU)-transformed BPH-1 series cell lines into the dorsal lateral flank. Tumors were allowed to grow, measured weekly with calipers, and tumor volumes were calculated using the formula $0.532 \times r1^2 \times r2$ ($r1 < r2$). Mice were weighed every week. Once they reached the endpoint (tumor size > 1 cm^3), mice from all groups were euthanized by CO_2 and cervical dislocation.

Gene profiling

After NMU-induced transformation was completed, gene expression profiles were identified by the Oligo GEArray Human Cancer Microarray (SABioscience) according to manufacturer's manual. Briefly, RNA harvested from cells was used as template for generating biotin-labeled probes. After hybridization of membranes containing cancer pathway-related genes with probes, membranes were washed and then developed for chemiluminescence imaging (VersaDoc, BioRad). After analysis using SABioscience online quantification software, genes with expression altered ≥ 1.5-fold were identified. By using GoMiner online software, altered genes between groups were functionally categorized and analyzed for statistical significance ($P < 0.05$).

GFP-based NHEJ and HR assay

These assays are described in the literature for NHEJ (25) and HR reporter assay (26). In brief, for NHEJ assay, BPH-1 cells were treated with EtOH or 1,25-VD for 24 hours and then transfected with GFP expression plasmids (*HindIII* digested; 0.5 μg/10^5 cells) that express GFP only after repair of digested breaks and pDsRed-N1 (0.5 μg/10^5 cells) for transfection control. Cells were harvested 2 days after transfection. The efficiency of NHEJ repair was analyzed using flow cytometry to quantify GFP-positive cells, which represent successful NHEJ DNA repair, and normalized by DsRed-positive cells for transfection efficiency. For HR assay, BPH-1 cells were treated as described above and transfected with plasmids for homologous recombination assay (pDR-GFP and pCβASce, both at 0.5 μg/10^5 cells). Cells transfected with pDR-GFP plasmid were selected by puromycin (2 μg/mL) for 2 days and then harvested at 6 days after transfection. Cells were subjected to analysis of GFP-positive cells under flow cytometry. Transfection was conducted by the Neon Transfection System (Invitrogen). Flow cytometry was carried out using FACSCanto-II (BD) and analyzed by FlowJo software.

Establishing siRNA-targeted VDR knockdown stable cell lines

Retrovirus-based plasmids (pSM2c) carrying siRNA-targeting VDR (siVDR) and control siRNA (SC) were purchased from Open Biosystem. Stable cell lines expressing these siRNAs were generated according to the manufacturer's manual (OligoEngine).

Chromatin immunoprecipitation assay

Chromatin immunoprecipitation assays were conducted according to a previous publication (27). DNA fragments containing VDREs in *ATM* and *RAD50* genes were amplified by specific primer pairs (sequence available upon request).

In vitro kinase assay

ATM kinase assay was conducted according to a previous publication (28). Glutathione *S*—transferase (GST)-conjugated VDR fragment proteins were isolated according to the manufacturer's manual (Promega).

Immunoprecipitation and detection of phosphoserine

BPH-1 cells on 10-cm dishes were treated with KU55933 for 2 hours and then exposed to 1 mmol/L H_2O_2 for 30 minutes and then changed to fresh normal medium. Proteins were harvested 3 hours after H_2O_2 challenge by radioimmunoprecipitation assay (RIPA) buffer containing protease inhibitor (cOmplete mini; Roche) and phosphatase inhibitor (1 mmol/L NaF and 1 mmol/L $NaVO_3$). Proteins were incubated with anti-VDR overnight at 4°C, precipitated by protein A/G agarose beads (Santa Cruz), washed 3 times with RIPA buffer and then loaded on 12% SDS-PAGE. Phosphoserine was detected by Western blotting using anti-phosphoserine and peroxidase-IgG fraction monoclonal mouse anti-rabbit IgG, light chain specific (Jackson ImmunoResearch Lab).

Cell viability assay, quantitative PCR analysis, Western blotting assay, transient transfection and luciferase assays, and DNA pull-down assay

Cell viability assay, quantitative PCR (Q-PCR) analysis, Western blotting assay, transient transfection and luciferase assays, and DNA pull-down assays were conducted according to previous publications (27, 29). Sequence of oligomers for amplifying *actin, ATM,* and *RAD50* in Q-PCR assay are available upon request.

Results

Vitamin D is chemopreventive in NMU transformation model

To further investigate the chemopreventive effect of vitamin D supplementation, an *in vitro* model using NMU to transform prostate epithelial cells was applied (30). BPH-1 cells, a nonmalignant human prostate epithelial cell line (31), were subjected to 3 repeated cycles of NMU treatment and then subcultured for another 6 passages to select clones with significant growth advantage (Fig. 1A).

In an anchorage-independent colony-forming assay, BPH-1 (NMU) cells formed many colonies indicating malignant transformation (Fig. 1B, middle). Importantly, 1,25-VD treatment can reduce NMU-induced BPH-1 malignant transformation with fewer colonies formed (Fig. 1B, bottom). The tumorigenicity was further confirmed in xenografted nude mice. The result showed that 60% of NMU-treated BPH-1 cells formed tumors ($n = 10$), but none of the dimethyl sulfoxide (DMSO)-treated BPH-1 cells ($n = 16$) or 1,25-VD-pretreated NMU-BPH-1 cells ($n = 6$) formed growing tumors (Fig. 1C). Tumor forming frequency between BPH-1 (NMU) and BPH-1 (VD + NMU) is 60% versus 0% ($P = 0.034$; Fisher exact test).

DNA damage signaling genes and DNA repair are promoted by 1,25-VD

To investigate the underlying molecular mechanism, we conducted gene profiling analysis using the human Cancer Pathway SuperArray (Supplementary Fig. S1A). We found that 63 genes were altered at a magnitude ≥1.5-fold by vitamin D in the NMU-treated groups, including 23 upregulated and 40 downregulated among a total of 440 genes. These genes were distributed in 4 statistically significant Gene Ontology (GO) categories (Supplementary Fig. S1B).

Two DSB repair genes, *ATM* and *RAD50,* were found to express higher in BPH-1 (VD + NMU) than in BPH-1 (NMU; Supplementary Fig. S1B and S1C). We suspected that 1,25-VD promotes or maintains DNA DSB damage repair capacity that is altered by carcinogen and other genotoxic challenges. We examined whether 1,25-VD treatment can also promote cell recovery from NMU-induced DSB by a γ-H2Ax kinetic assay. Although NMU generates DNA alkylation that is repaired mostly by base excision repair, it is also known that DSB occurs upon alkylating reagents challenge (32) and that DSB repair protects cells from genotoxicity of alkylating agents (33). We found that NMU exposure increased the levels of γ-H2Ax starting from 30 minutes, to a maximum at 2 hours in vehicle-treated cells, but the NMU-induced γ-H2Ax induction was significantly reduced in the 1,25-VD-treated cells (Fig. 2A). Measuring γ-H2Ax foci number found that 1,25-VD can reduce NMU-induced foci numbers at 2 hours after NMU exposure (Fig. 2B). This was not due to 1,25-VD altering cell-cycle distribution (Supplementary Fig. S2A). We also observed that the protective effect of 1.25-VD in H_2O_2 induced DSB at 6 hours (Supplementary Fig. S2B). These findings that γ-H2Ax foci numbers and ATM activation (Supplementary Fig. S2C) by genotoxic insults were lower in 1,25-VD-treated groups suggest that 1,25-VD decreased DSB levels. RWPE-1 is another nonmalignant prostate epithelial cell line in which the DNA-protective effects of 1,25-VD were also observed (Supplementary Fig. S3). This could be a result of 1,25-VD reducing ROS generation as shown in our previous publication (29) and/or promoting DSB DNA repair when cells are faced with genotoxic insults.

To further understand whether 1,25-VD can promote DSB DNA repair, we examined the effects of 1,25-VD on 2 DSB repair pathways: NHEJ and HR repair. Treatment of BPH-1 cells with 1,25-VD significantly promoted the HR DNA repair capacity, as well as the NHEJ DNA repair capacity but to a lesser degree (Fig. 2C). Together, these results suggested that 1,25-VD protects cells from genotoxic insults through inducing DNA repair genes' expression to promote the repair of DSB.

VDRs protect cells from genotoxicity and tumorigenesis

To explore whether VDR mediates the protective role of 1,25-VD against genotoxicity, we established siRNA VDR knocked down (BPH-1siVDR) versus scramble control (BPH-1SC) BPH-1 cell lines. VDR knockdown efficiency was 70% and VDR transactivity measured by the induction of *CYP24, ATM,* and *RAD50* expression was reduced (Fig. 3A). The protective effect of 1,25-VD against H_2O_2 and IR-induced cell death was lost in BPH-1siVDR cells compared with BPH-1SC cells (Fig. 3B; Supplementary Fig. S4A). Moreover, the effect of 1,25-VD facilitating DSB recovery could only be seen in BPH-1SC but not in BPH-1siVDR cells (Fig. 3C). All these data support role of VDR in protecting cells from genotoxicity.

Next, we examined the role of VDR in the chemopreventive effect of 1,25-VD. Knockdown of VDR sufficiently induced colony formation, representing tumorigenicity, even without NMU treatment (Fig. 3D, DMSO-treated BPH-1siVDR vs. BPH-1SC). This is observed from 2 independent stable clones and is therefore unlikely to result from insertion of transgenes into critical genome sites. This result strongly supports the tumor-suppressive role of VDR. However, 1,25-VD treatment can still reduce NMU-induced tumorigenicity in

BPH-1siVDR cells. (The representative photos of colonies are shown in Supplementary Fig. S4B.)

These results suggest that 1,25-VD has VDR-independent chemopreventive effects or can still function through the residual VDR signal amplified by ATM-VDR signaling loop during carcinogen challenges. To clarify whether VDR is essential in mediating the chemopreventative effect of 1,25-VD, we obtained VDR-null MEFs from VDR knockout mice (VDRko) to examine whether 1,25-VD can still suppress the tumorigenesis process in the absence of VDR. At the eleventh passage, VDRko MEFs spontaneously formed colonies in soft agar assays whereas VDR heterozygous deletion (VDRhet) MEFs formed very few colonies. Treatment of 1,25-VD cannot suppress VDRko MEFs from gaining colony-forming ability (Fig. 3E; Supplementary Fig. S4C). This supports the tumor-suppressive role of VDR and suggests that the tumor-suppressive effect of 1,25-VD requires the presence of VDR.

ATM phosphorylates and actives VDR transactivity

ATM kinase is a key molecule that senses DSB and then activates the DDR signaling cascade. H_2O_2 exposure quickly activates ATM within 30 minutes at concentrations starting at 0.1 mmol/L (Supplementary Fig. S5A). Interestingly, we observed that the 1,25-VD-induced VDR transactivity was further enhanced by H_2O_2 challenge (Supplementary Fig. S5B and S5C).

To test whether VDR is a downstream target of DDR signaling kinases upon induction of genotoxic stress stimuli, we screened for the phosphorylation motif on VDR using the web tool Scansite (http://scansite.mit.edu/). Three putative ATM target sites were identified (Fig. 4A).

In vitro kinase assays revealed that ATM phosphorylated the VDR-L and VDR-L1 fragments both containing s208 and s222 but not the VDR-L2 (Fig. 4B, bottom). In the sample containing ATM and VDR-L1, 3 phosphorylated bands were found including ATM, VDR-L1 (*), and an unknown band (#) that might be degraded VDR. ATM autophosphorylation and BRCA1 phosphorylation bands were observed as positive control.

We further mutated the putative phosphorylation sites in GST-VDR-L and GST-VDR-L1 fragment to generate GST-dmVDR-L and GST-dmVDR-L1. The result showed that the phosphorylation was reduced but not completely abolished in these mutated fragments. VDR transactivation activity was enhanced by ATM but not by ATM dead mutant (ATMkd; Fig. 4C). The single serine-mutated VDRs (VDRs208g and VDR s222a) and double serine mutant VDR (dmVDR) can respond to 1,25-VD-induced transactivity (Fig. 4C). However, only the dmVDR completely lost response to ATM (Fig. 4C). These results indicate that ATM enhances VDR activity through phosphorylation of 2 amino acids, ser208 and ser222. Similarly, overexpression of ATM promotes endogenous VDR transactivity in BPH-1 cells (Fig. 4D).

We next found that ATM-specific inhibitor, KU55933, inhibited H_2O_2-enhanced VDR phosphorylation and transactivity (Fig. 4E and F). Therefore, DNA damage induced

phosphorylation and transactivation of VDR through ATM. We further compared the DNA-binding ability of VDR and dmVDR. The result showed that H_2O_2 and 1,25-VD induced DNA binding ability of wild-type (wt) VDR. On the other hand, dmVDR bound VDRE but did not respond to 1,25-VD and H_2O_2 stimulation as strongly as wtVDR (Fig. 4G). Taken together, these data suggest that DNA damage signals enhance VDR activity through phosphorylation at s208 and s222 by ATM.

ATM-modified VDR is required for VDR cellular protective effects against H_2O_2 challenge

On the basis of our results showing that 1,25-VD treatment can protect cells against DNA damage insult (Fig. 2) and VDR is a downstream target of the ATM cascade (Fig. 4), we then hypothesized that DNA-protective effect of 1,25-VD-VDR is modulated by ATM, such that phosphorylation of VDR by ATM is critical for this protective effect.

To test this hypothesis, we compared cell survival upon H_2O_2 challenge in cells overexpressing wtVDR and dmVDR. Because the transactivity of dmVDR cannot be stimulated by ATM (Fig. 4C), dmVDR serves as a tool to delineate the cellular function of ATM-phosphorylated VDR. BPH-1 cells were transiently overexpressed with wtVDR or dmVDR, treated with 1,25-VD for 24 hours, and then exposed to H_2O_2 to determine cell survival. The results showed that cell survival was increased in BPH-1 cells overexpressing wtVDR and treatment with 1,25-VD promoted cell survival.

In contrast, cells overexpressing dmVDR had a similar basal survival rate as compared with vector control cells (EtOH group) but the protective effect of 1,25-VD was lost in these dmVDR cells (Fig. 5A). The overexpression level of wtVDR and dmVDR mRNA and proteins were confirmed to be equivalent (Fig. 5B). In addition, we examined the expression of *RAD50* induced by 1,25-VD in cells expressing various types of VDR. The expression of *ATM* and *RAD50* was induced by 1,25-VD in BPH-1 (vector) cells and further induced in BPH-1 (VDR) cells which were overexpressed with wtVDR. Interestingly, the induction of *ATM* and *RAD50* by 1,25-VD is abolished in the BPH-1 (dmVDR) cells (Fig. 5C).

To further validate that ATM-phosphorylated VDR is critical for 1,25-VD protective effect against genotoxicity, the different VDRs (wt vs. dmVDR) were reexpressed in BPH-1siVDR cells (Fig. 5D). The result showed that 1,25-VD has no protective effect on BPH-1siVDR cells (Fig. 5D, left), and wtVDR reexpression rescued the protective effect of 1,25-VD (middle) but not dmVDR (right). In summary, we conclude that activation of VDR by ATM phosphorylation is essential for the DNA-protective effect of 1,25-VD and this 1,25-VD/VDR protective effect provides one functional mechanism mediating antitumorigenic effect of vitamin D.

Discussion

Here, we investigate the mechanisms underlying the chemopreventive effect of vitamin D in tumorigenesis. These results show that 1,25-VD treatment can protect cells from carcinogen-induced genotoxic stress via VDR-mediated transcriptional upregulation of DNA repair genes, *ATM* and *RAD50,* and thereby facilitate DSB repair. Reciprocally, DDR signaling kinase ATM phosphorylates and enhances the transactivity of VDR. Figure 6 illustrates that

activation of the ATM-VDR-positive signaling loop upon carcinogen/oncogenic stress contributes to the protective effect of 1,25-VD against genomic insult-induced cell death and malignant transformation.

Currently, the effect of vitamin D supplementation in human cancer prevention is still under evaluation. One major concern for using vitamin D supplements in tumor prevention is the hypercalcemia side effect due to high dosage vitamin D uptake. In this study, we found that a high concentration of 1,25-VD (100 nmol/L) is required to prevent BPH-1 from malignant transformation. It is estimated that more than 4,000 IU/kg vitamin D supplement is required to reach such dosage. However, the current physiologic recommended upper limit dosage of vitamin D supplementation is 2,000 IU. One possibility for this high dosage requirement in BPH-1 is that it is immortalized by SV40 T antigens which disrupts vitamin D signaling pathways by squelching p53 and/or downregulating VDR expression (34, 35). We predict that the physiologic concentration of 1,25-VD will be sufficient to activate the antitumorigenic effect of VDR in normal cells that contain functional p53 and Rb. Therefore, the optimal dosage of vitamin D supplement required for preventing cancer needs to be further studied.

Phosphorylation of ATM putative target sites, s208 and s222, in VDR can enhance VDR transactivity and that mutation of both serines in VDR (dmVDR) impairs ATM-VDR signaling loop. ATM enhances VDR transactivity by increasing the DNA-binding ability of VDR as evidenced by VDRE-binding studies showing that genotoxic stress induces VDR-VDRE complexes of wtVDR but not of dmVDR (Fig. 4G; Supplementary Fig. S5C). As stated in the literature, casein kinase II can also phosphorylate VDR s208 (36). Phosphorylation of VDR s208 does not affect ligand binding, DNA binding, or RXR heterodimerization of VDR but does promote the recruitment of DRIP205 as noted by the enhancement of VDR transactivity (36, 37). Therefore, we expect that DRIP205 recruitment is another mechanism by which ATM enhances VDR transactivity.

The positive regulatory loop constituted by ATM-VDR led us to predict that 1,25-VD treatment will act synergistically with DDR signaling in suppressing tumorigenesis. Our study showed that once the ATM-VDR loop is broken by either siVDR or dmVDR, the 1,25-VD regulation of ATM and RAD50 expression and protective effect of 1,25-VD against genotoxic challenges are lost (Figs. 3 and 5). These results support a critical role of the intact ATM-VDR loop in mediating DNA-protective effect of vitamin D. Interestingly, the chemopreventive effect of 1,25-VD is not abolished by siVDR (Fig. 3). This suggests the DNA-protective effect of 1,25-VD might not be the only chemopreventive mechanism of 1,25-VD. Other cancer pathways identified in array can also contribute to the anti-tumorigenic effect of 1,25-VD (Supplementary Fig. S1B). Remaining ATM-VDR signaling is possibly sufficient in mediating 1,25-VD regulation of other cancer pathways. Indeed, complete depletion of VDR by using VDRko MEF abolishes the tumor-suppressive effect of 1,25-VD. This supports the essential role of ATM-VDR loop in mediating the antitumorigenic effect of vitamin D. In addition, we challenged MEFs with NMU (3 cycles and one passage) but failed to induce more colonies (data not shown). More passages might be required to enrich the malignant population to examine the chemopreventive effect of vitamin D during carcinogen-induced malignant transformation. Meanwhile, we also

immortalized MEFs by SV40LT. Interestingly, these immortalized MEFs from VDRko and VDRhet form colonies spontaneously. Once MEFs are being transformed by SV40LT, vitamin D is no longer able to reduce their colony-forming ability (data not shown). Therefore, cells should be treated with vitamin D prior malignant transformation to show its chemopreventive activity. On the other hand, we expect that if ATM-phosphorylated VDR is constitutively expressed, the chemopreventive effect of 1,25-VD could be amplified. Exploiting the ATM-VDR signaling loop by combination of 1,25-VD and ATM activators is therefore potentially a novel strategy to prevent cancer while mitigating the hypercalcemia side effects of vitamin D.

Overall, our efforts in mechanistic studies support the role of vitamin D in guarding genomic integrity through regulation of genes involved in anti-oxidation (29) and DNA repair. Other potential pathways including inducing Ras signaling and suppressing antiapoptotic genes demand future study. Another gene profiling study of 1,25-VD-treated RWPE-1 cells identifies the WNT, Notch, NF-κB, insulin—like growth factor 1, and inflammation signaling, those are also potential chemopreventive mechanisms of 1,25-VD worth pursuing (38). In patients with cancer, the DNA-protective effect of vitamin D can compromise the efficacy of therapies targeting DNA, such as radiotherapy and chemotherapy. Therefore, the status of vitamin D signaling, including the availability of ligands and receptor, could serve as a prognostic biomarker for predicting the response of patients to radiotherapy and chemotherapy. On the other hand, vitamin D supplementation might be one supportive treatment for protection against DNA damage caused by radiation exposure in healthy individuals. Finally, a novel vitamin D-based chemopreventive strategy could be developed on the basis of the ATM-VDR-positive signaling loop.

Supplementary Material

Refer to Web version on PubMed Central for supplementary material.

References

1. Garland C, Shekelle RB, Barrett-Connor E, Criqui MH, Rossof AH, Paul O. Dietary vitamin D and calcium and risk of colorectal cancer: a 19-year prospective study in men. Lancet 1985;1:307–9. [PubMed: 2857364]
2. Garland FC, Garland CF, Gorham ED, Young JF. Geographic variation in breast cancer mortality in the United States: a hypothesis involving exposure to solar radiation. Prev Med 1990;19: 614–22. [PubMed: 2263572]
3. Schwartz GG, Hulka BS. Is vitamin D deficiency a risk factor for prostate cancer? (Hypothesis). Anticancer Res 1990;10:1307–11. [PubMed: 2241107]
4. Garland CF, Comstock GW, Garland FC, Helsing KJ, Shaw EK, Gorham ED. Serum 25-hydroxyvitamin D and colon cancer: eight-year prospective study. Lancet 1989;2:1176–8. [PubMed: 2572900]
5. Ahonen MH, Tenkanen L, Teppo L, Hakama M, Tuohimaa P. Prostate cancer risk and prediagnostic serum 25-hydroxyvitamin D levels (Finland). Cancer Causes Control 2000;11:847–52. [PubMed: 11075874]
6. Corder EH, Guess HA, Hulka BS, Friedman GD, Sadler M, Vollmer RT, et al. Vitamin D and prostate cancer: a prediagnostic study with stored sera. Cancer Epidemiol Biomarkers Prev 1993;2:467–72. [PubMed: 8220092]

7. Wood AW, Chang RL, Huang MT, Uskokovic M, Conney AH. 1 alpha, 25-Dihydroxyvitamin D3 inhibits phorbol ester-dependent chemical carcinogenesis in mouse skin. Biochem Biophys Res Commun 1983;116:605–11. [PubMed: 6689123]
8. Kawaura A, Tanida N, Nishikawa M, Yamamoto I, Sawada K, Tsujiai T, et al. Inhibitory effect of 1alpha-hydroxyvitamin D3 on N-methyl-N'-nitro-N-nitrosoguanidine-induced gastrointestinal carcinogenesis in Wistar rats. Cancer Lett 1998;122:227–30. [PubMed: 9464515]
9. Lucia MS, Anzano MA, Slayter MV, Anver MR, Green DM, Shrader MW, et al. Chemopreventive activity of tamoxifen, N-(4-hydroxyphenyl) retinamide, and the vitamin D analogue Ro24–5531 for androgen-promoted carcinomas of the rat seminal vesicle and prostate. Cancer Res 1995;55:5621–7. [PubMed: 7585644]
10. Zinser GM, Suckow M, Welsh J. Vitamin D receptor (VDR) ablation alters carcinogen-induced tumorigenesis in mammary gland, epidermis and lymphoid tissues. J Steroid Biochem Mol Biol 2005;97: 153–64. [PubMed: 16111884]
11. De Haes P, Garmyn M, Verstuyf A, De Clercq P, Vandewalle M, Degreef H, et al. 1,25-Dihydroxyvitamin D3 and analogues protect primary human keratinocytes against UVB-induced DNA damage. J Photo-chem Photobiol B 2005;78:141–8.
12. Wong G, Gupta R, Dixon KM, Deo SS, Choong SM, Halliday GM, et al. 1,25-Dihydroxyvitamin D and three low-calcemic analogs decrease UV-induced DNA damage via the rapid response pathway. J Steroid Biochem Mol Biol 2004;89–90:567–70.
13. Chatterjee M Vitamin D and genomic stability. Mutat Res 2001;475: 69–87. [PubMed: 11295155]
14. Hanada K, Sawamura D, Nakano H, Hashimoto I. Possible role of 1,25-dihydroxyvitamin D3-induced metallothionein in photoprotection against UVB injury in mouse skin and cultured rat keratinocytes. J Dermatol Sci 1995;9:203–8. [PubMed: 8664218]
15. De Haes P, Garmyn M, Degreef H, Vantieghem K, Bouillon R, Segaert S. 1,25-Dihydroxyvitamin D3 inhibits ultraviolet B-induced apoptosis, Jun kinase activation, and interleukin-6 production in primary human keratinocytes. J Cell Biochem 2003;89:663–73. [PubMed: 12858333]
16. Banakar MC, Paramasivan SK, Chattopadhyay MB, Datta S, Chakraborty P, Chatterjee M, et al. 1alpha, 25-dihydroxyvitamin D3 prevents DNA damage and restores antioxidant enzymes in rat hepatocarcinogenesis induced by diethylnitrosamine and promoted by phenobarbital. World J Gastroenterol 2004;10:1268–75. [PubMed: 15112340]
17. Krishnan AV, Shinghal R, Raghavachari N, Brooks JD, Peehl DM, Feldman D. Analysis of vitamin D-regulated gene expression in LNCaP human prostate cancer cells using cDNA microarrays. Prostate 2004;59:243–51. [PubMed: 15042599]
18. Wu-Wong JR, Nakane M, Ma J, Ruan X, Kroeger PE. Effects of Vitamin D analogs on gene expression profiling in human coronary artery smooth muscle cells. Atherosclerosis 2006;186:20–8. [PubMed: 16095599]
19. O'Driscoll M, Jeggo PA. CsA can induce DNA double-strand breaks: implications for BMT regimens particularly for individuals with defective DNA repair. Bone Marrow Transplant 2008;41:983–9. [PubMed: 18278071]
20. Takata M, Sasaki MS, Sonoda E, Morrison C, Hashimoto M, Utsumi H, et al. Homologous recombination and non-homologous end-joining pathways of DNA double-strand break repair have overlapping roles in the maintenance of chromosomal integrity in vertebrate cells. EMBO J 1998;17:5497–508. [PubMed: 9736627]
21. Hoeijmakers JH. Genome maintenance mechanisms for preventing cancer. Nature 2001;411:366–74. [PubMed: 11357144]
22. Park Y, Gerson SL. DNA repair defects in stem cell function and aging. Annu Rev Med 2005;56:495–508. [PubMed: 15660524]
23. Bartkova J, Horejsi Z, Koed K, Kramer A, Tort F, Zieger K, et al. DNA damage response as a candidate anti-cancer barrier in early human tumorigenesis. Nature 2005;434:864–70. [PubMed: 15829956]
24. Bartkova J, Rezaei N, Liontos M, Karakaidos P, Kletsas D, Issaeva N, et al. Oncogene-induced senescence is part of the tumorigenesis barrier imposed by DNA damage checkpoints. Nature 2006;444: 633–7. [PubMed: 17136093]

25. Seluanov A, Mittelman D, Pereira-Smith OM, Wilson JH, Gorbunova V. DNA end joining becomes less efficient and more error-prone during cellular senescence. Proc Natl Acad Sci U S A 2004;101:7624–9. [PubMed: 15123826]
26. Pierce AJ, Johnson RD, Thompson LH, Jasin M. XRCC3 promotes homology-directed repair of DNA damage in mammalian cells. Genes Dev 1999;13:2633–8. [PubMed: 10541549]
27. Ting HJ, Bao BY, Reeder JE, Messing EM, Lee YF. Increased expression of corepressors in aggressive androgen-independent prostate cancer cells results in loss of 1alpha,25-dihydroxyvitamin D3 responsiveness. Mol Cancer Res 2007;5:967–80. [PubMed: 17855664]
28. Kim ST, Lim DS, Canman CE, Kastan MB. Substrate specificities and identification of putative substrates of ATM kinase family members. J Biol Chem 1999;274:37538–43. [PubMed: 10608806]
29. Bao BY, Ting HJ, Hsu JW, Lee YF. Protective role of 1 alpha, 25-dihydroxyvitamin D3 against oxidative stress in nonmalignant human prostate epithelial cells. Int J Cancer 2008;122:2699–706. [PubMed: 18348143]
30. Rhim JS, Jin S, Jung M, Thraves PJ, Kuettel MR, Webber MM, et al. Malignant transformation of human prostate epithelial cells by N-nitroso-N-methylurea. Cancer Res 1997;57:576–80. [PubMed: 9044828]
31. Hayward SW, Dahiya R, Cunha GR, Bartek J, Deshpande N, Narayan P. Establishment and characterization of an immortalized but non-transformed human prostate epithelial cell line: BPH-1. In Vitro Cell Dev Biol Anim 1995;31:14–24. [PubMed: 7535634]
32. Staszewski O, Nikolova T, Kaina B. Kinetics of gamma-H2AX focus formation upon treatment of cells with UV light and alkylating agents. Environ Mol Mutagen 2008;49:734–40. [PubMed: 18800352]
33. Tsaryk R, Fabian K, Thacker J, Kaina B. Xrcc2 deficiency sensitizes cells to apoptosis by MNNG and the alkylating anticancer drugs temozolomide, fotemustine and mafosfamide. Cancer Lett 2006;239: 305–13. [PubMed: 16298473]
34. Maruyama R, Aoki F, Toyota M, Sasaki Y, Akashi H, Mita H, et al. Comparative genome analysis identifies the vitamin D receptor gene as a direct target of p53-mediated transcriptional activation. Cancer Res 2006;66:4574–83. [PubMed: 16651407]
35. Kemmis CM, Welsh J. Mammary epithelial cell transformation is associated with deregulation of the vitamin D pathway. J Cell Biochem 2008;105:980–8. [PubMed: 18767073]
36. Jurutka PW, Hsieh JC, Nakajima S, Haussler CA, Whitfield GK, Haussler MR. Human vitamin D receptor phosphorylation by casein kinase II at Ser-208 potentiates transcriptional activation. Proc Natl Acad Sci U S A 1996;93:3519–24. [PubMed: 8622969]
37. Arriagada G, Paredes R, Olate J, van Wijnen A, Lian JB, Stein GS, et al. Phosphorylation at serine 208 of the 1alpha,25-dihydroxy Vitamin D3 receptor modulates the interaction with transcriptional coactivators. J Steroid Biochem Mol Biol 2007;103: 425–9. [PubMed: 17368182]
38. Kovalenko PL, Zhang Z, Cui M, Clinton SK, Fleet JC. 1,25 dihydroxyvitamin D-mediated orchestration of anticancer, transcript-level effects in the immortalized, non-transformed prostate epithelial cell line, RWPE1. BMC Genomics 2010;11:26. [PubMed: 20070897]

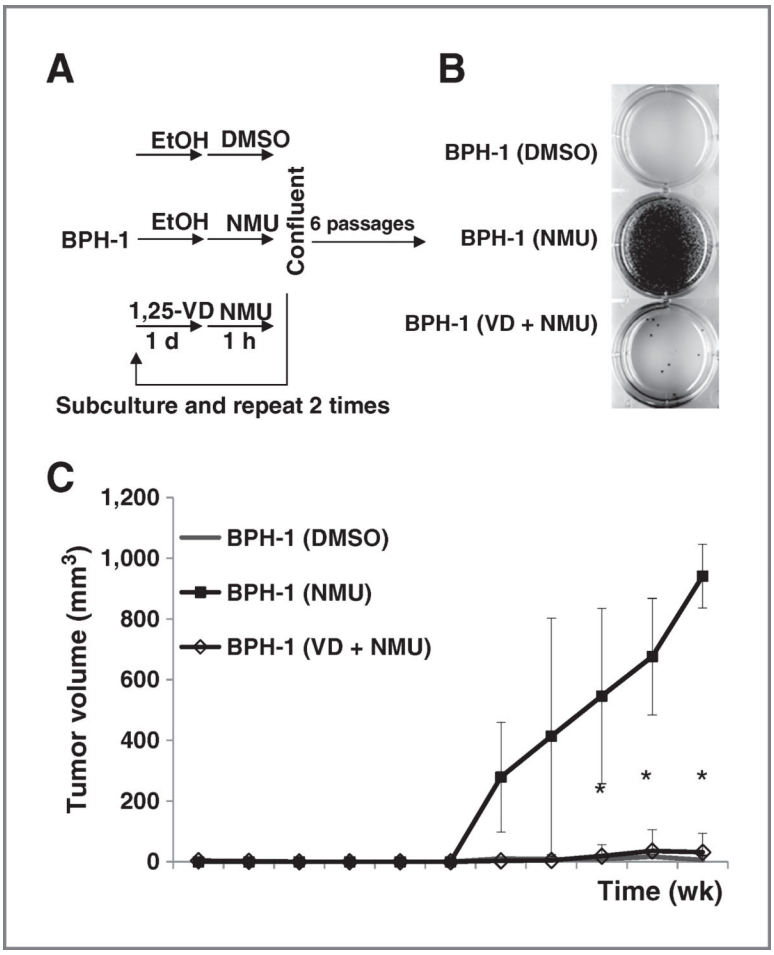

Figure 1.

Pretreatment with 1,25-VD prevented cell transformation. BPH-1 cells were seeded at 3×10^4 cells per dish in 60-mm dishes. A, diagram of NMU-induced transformation procedure. Cells were treated with ethanol (EtOH) or 100 nmol/L 1,25-VD for 24 hours and then exposed to 100 μg/mL NMU for 1 hour. The same treatment was repeated for another 2 times. After 6 times subculture, soft agar colony-forming assays were conducted. B, representative colony formation of cells with indicated treatment from triplicate experiments are shown. C, BPH-1 sublines at 10^6 cells per 100 μL Matrigel were subcutaneously injected into nude mice. Tumor volumes of BPH-1 (DMSO), BPH-1 (NMU),and BPH-1 (VD + NMU) groups were measured as described in Materials and Methods and mean ± SD of all xenograft tumors plotted. *, $P < 0.05$ BPH-1 (VD + NMU) cell xenograft tumors compared with BPH-1 (NMU) cell xenograft tumors.

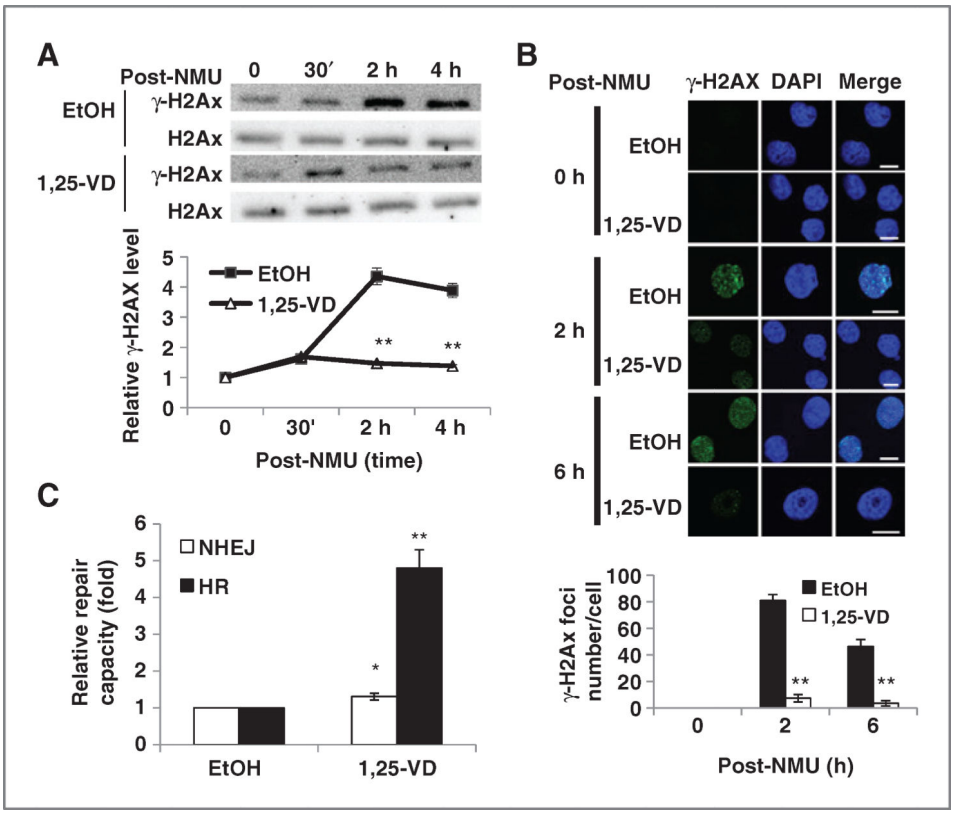

Figure 2.

1,25-VD protects cells from DSBs and promotes DSB DNA repair. A, 1,25-VD promotes cells' recovery from NMU-induced DSB. BPH-1 cells were Incubated with vehicle or 100 nmol/L 1,25-VD for 24 hours and then exposed to NMU (100 μg/mL) for 1 hour. DNA DSB marker γ-H2Ax was detected at designated time points by Western blotting. After being normalized with H2Ax, the relative intensity of γ-H2Ax to 0 hours was calculated and plotted. **, $P < 0.01$ compared with EtOH-treated group at the same time point. B, BPH-1 cells were seeded at 10^4 cells per well on chamber slide and then treated with EtOH or 100 nmol/L 1,25-VD the next day. After 24 hours, cells were treated with or without H_2O_2 (0.1 mmol/L) for 30 minutes and then replenished with fresh medium containing EtOH or 1,25-VD. Cells were fixed at indicated time points and processed for staining with an antibody for γ-H2Ax. Pictures were taken by confocal microscopy and representative pictures are shown (scale bar, 15 μm). γ-H2Ax foci numbers were counted and then average foci numbers per cell ± SD were plotted. **, $P < 0.01$. C, 1,25-VD promotes NHEJ and HR repair. BPH-1 cells were treated with EtOH or 100 nmol/L 1,25-VD for 24 hours and then cotransfected with *Hind*III-digested NHEJ reporter and DsRed-expressing vector (NHEJ assay) or pDR-GFP and PcβASce plasmids (homologous recombination assay). Cells were continuously treated with EtOH or 1,25-VD until harvest. The percentage of GFP^+ and $DsRed^+$ cells were determined by fluorescence-activated cell-sorting (FACS) analysis. The relative repair efficiency was calculated by comparing with EtOH-treated group. *, $P < 0.05$; **, $P < 0.01$, compared with EtOH group ($n = 3$). DAPI, 4′,6-diamidino-2-phenylindole.

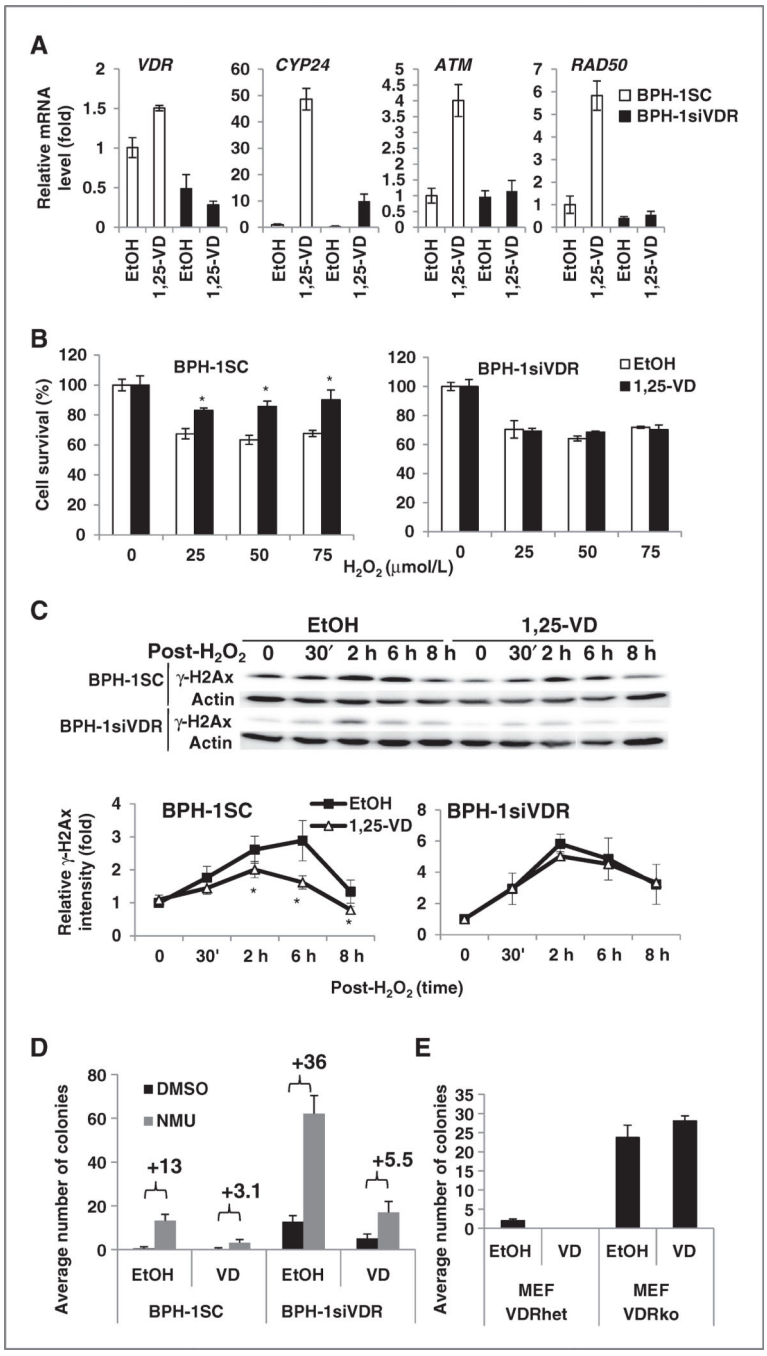

Figure 3.

The protective effect of 1,25-VD against genotoxic challenges in VDR-depleted cells. A, 1,25-VD induced gene expression in VDR-depleted cells. BPH-1SC and BPH-1siVDR cells were treated with EtOH or 100 nmol/L 1,25-VD for 24 hours and then harvested for RNA extraction. The expression of indicated genes was measured by Q-PCR. The relative expression compared with BPH-1SC treated with EtOH was calculated and mean ± SD plotted. B, the protective effect of 1,25-VD against genotoxicity in VDR-depleted cells. BPH-1SC and BPH-1siVDR cells were treated with 100 nmol/L 1,25-VD for 24 hours and

then exposed to different doses of H_2O_2. After 6 days, MTT assays were conducted. Percentages of surviving cells in each treatment group compared with no H_2O_2 exposure were calculated (*, $P < 0.05$ compared with EtOH with same dosage of H_2O_2-treated group; $n = 3$). C, the effects of 1,25-VD on genotoxic agent-induced DSBs. BPH-1SC or BPH-1siVDR cells were incubated with EtOH or 100 nmol/L 1,25-VD for 24 hours and then exposed to H_2O_2 (0.1 mmol/L) for 30 minutes. At designated time points, proteins were harvested for detecting γ-H2Ax level. The relative intensity of γ-H2Ax (normalized by actin) compared with 0 hours was calculated and plotted. *, $P < 0.05$ compared with EtOH-treated groups at the same time points. D, the chemopreventive effect of 1,25-VD in VDR-depleted cells. NMU-induced malignant transformation was conducted in BPH-1SC and BPH-1siVDR cells as in Fig. 1A. Soft agar colony formation assay was conducted for examining tumorigenicity. Colony numbers were counted and averaged from 9 different fields of each well under microscope at 50× magnification. Average colony numbers from 2 independent experiments of 2 independent clones of BPH-1SC and BPH-1siVDR stable cell lines were calculated and mean ± SD plotted. E, MEF cells from VDRhet and VDRko mice were analyzed for their tumorigenicity after EtOH or 100 nmol/L 1,25-VD treatment for 24 hours three times. Colony numbers were counted and accumulated from 10 different fields of each well under microscope. Average colony numbers from 3 independent counting were calculated and mean ± SD plotted.

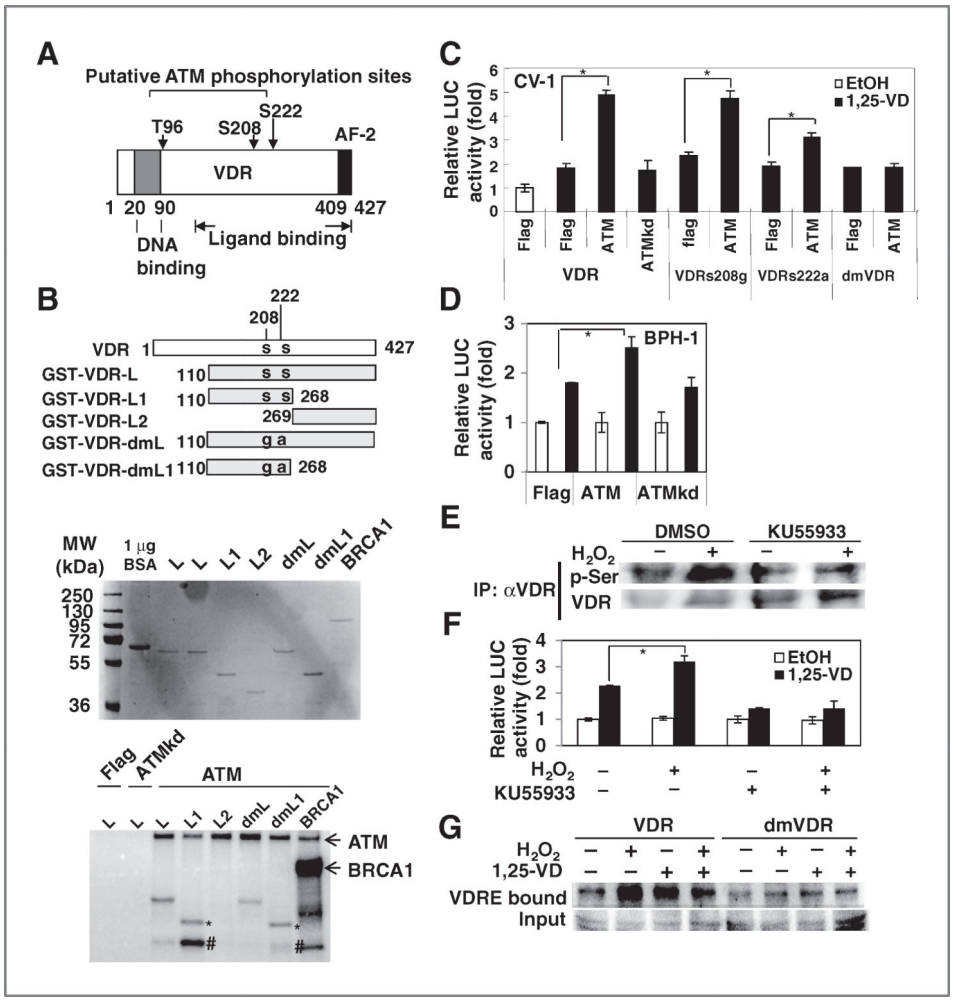

Figure 4.

ATM enhanced VDR transactivity through phosphorylation. A, illustration of 3 potential ATM phosphorylation sites on VDR (AF-2, activation function domain 2). B, ATM-phosphorylated VDR fragment containing s208 and s222. GST-VDR fragments (designed as in diagram, s, serine; g, glycine; a, alanine) and GST-BRCA1 fragments were expressed and purified from bacteria (top). Flag-ATM and Flag-ATMkd were expressed in 293T cells, immunoprecipitated (IP) by M2-agarose beads and then incubated with purified GST proteins in the presence of [γ−^{32}P]ATP. After reaction, samples were separated by electrophoresis, and phosphorylated proteins were detected by phosphorimager (bottom). Three independent experiments were carried out and the representative result is shown. (*, GST-VDR-L; #, possibly degraded GST-VDR-L). C, CV-1 cells were cotransfected with wt VDR or mutant VDRs, ATM, or ATMkd expression plasmids together with prCYP24-LUC. After overnight transfection, EtOH or 10 nmol/L 1,25-VD was added for another 24 hours. Cells were harvested for luciferase (LUC) assay. The relative LUC activity compared with VDR + Flag + EtOH group was calculated and mean ± SD plotted. *, $P < 0.05$ ($n > 3$). D, BPH-1 cells were cotransfected with ATM or ATMkd expression plasmids (0.6 μg) together with prCYP24-LUC (0.2 μg) per well of 24-well plate. After overnight transfection, EtOH or 100 nmol/L 1,25-VD was added for another 24 hours. Cells were harvested for LUC assay.

The relative LUC activity compared with EtOH group was calculated and mean ± SD plotted. *, $P < 0.05$ ($n = 3$). E, BPH-1 cells were treated with DMSO or KU55933 (10 μmol/L) for 2 hours and then exposed to H_2O_2 (1 mmol/L). VDR was immunoprecipitated by antibody and then p-Ser and VDR were detected by Western blotting. F, BPH-1 cells were transfected with pCYP24-LUC and pRL-SV40 and allowed to recover for 16 hours. Cells were then treated with DMSO or KU55933 for 2 hours and then exposed to 0.1 mmol/L H_2O_2 for 30 minutes, washed, and allowed to recover for indicated times and then treated with 1,25-VD for 24 hours for LUC assay. The relative LUC activity compared with EtOH group was calculated and mean ± SD plotted ($n > 3$). *, $P < 0.05$. G, BPH-1siVDR cells were transfected with VDR, wt or mutant, by electroporation. Cells were treated with or without 1 mmol/L H_2O_2 for 30 minutes and changed to fresh medium. After 2 hours, cells were treated with 1,25-VD (100 nmol/L) for 2 hours before harvesting proteins. VDR/VDRE complex were pulled down and VDR was detected by Western blotting. VDR input amounts were detected in 30% input proteins of each sample.

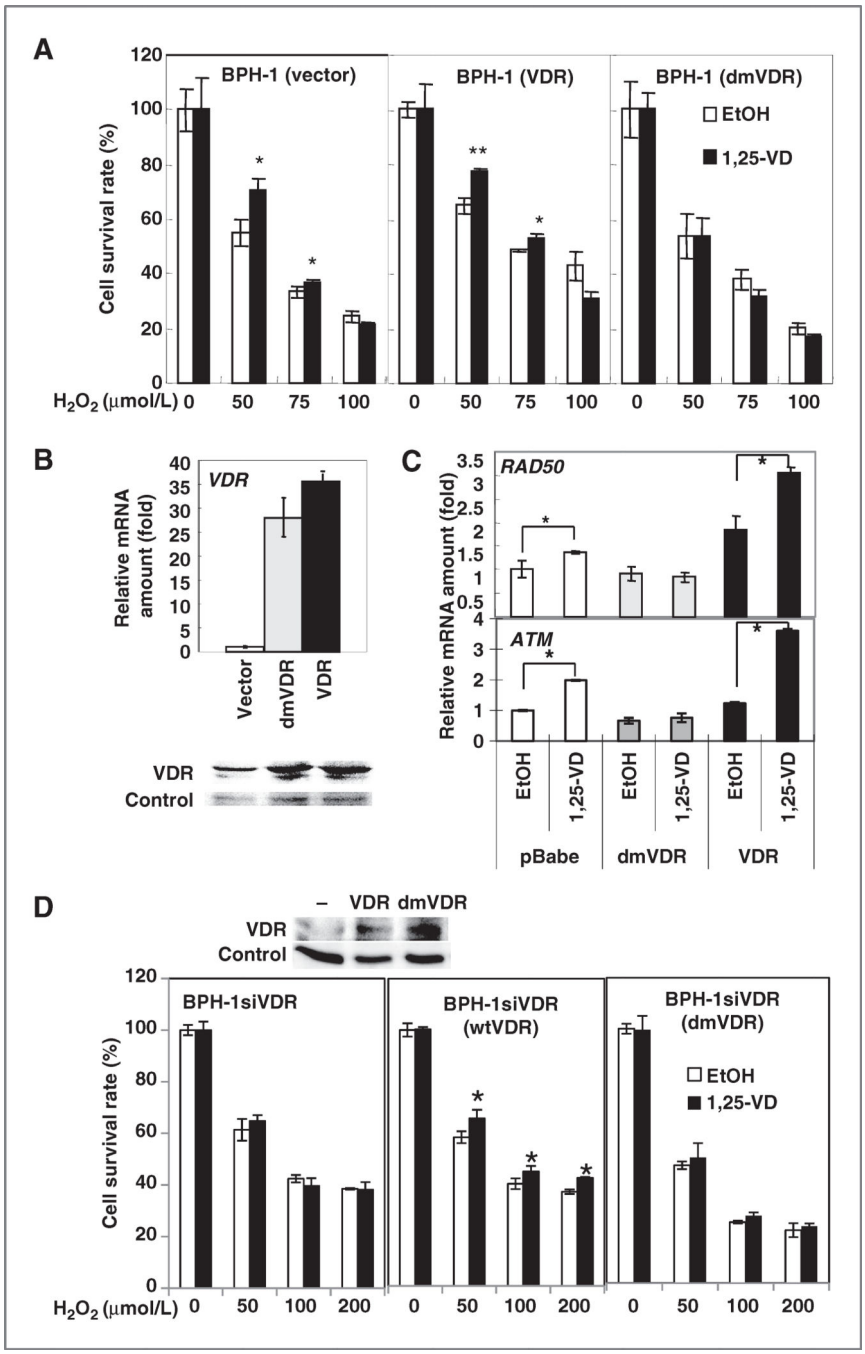

Figure 5.

The protective effect of 1,25-VD was lost in cells expressing dmVDR. A, BPH-1 cells were transfected with vector, wtVDR, or dmVDR-expressing vectors. After 1,25-VD treatment for 24 hours, cells were exposed to different concentrations of H_2O_2. Surviving cells were measured by MTT assay. The survival cell percentages relative to no H_2O_2 treatment were calculated and mean ± SD plotted. *, $P < 0.5$; **, $P < 0.01$ ($n = 3$). B, BPH-1 cells were infected with retrovirus carrying control vector, dmVDR, or wtVDR-expressing vector. The expression of VDR was measured by Q-PCR (top) and Western blotting (bottom). The

relative mRNA expression level of *VDR* compared with BPH-1 (vector) was calculated and mean ± S.D. plotted. C, transfected cells were treated with EtOH or 100 nmol/L 1,25-VD for 24 hours. The expression of *ATM* and *RAD50* mRNA was measured by Q-PCR. The relative expression compared with BPH-1 (vector) treated with EtOH was calculated and mean ± SD plotted. *, $P < 0.05$ ($n = 3$). D, as described in A, the protective effect of 1,25-VD in wt or dmVDR-overexpressed BPH-1siVDR cells was examined. *, $P < 0.5$ ($n = 3$). The protein level of VDR in parental and wtVDR or dmVDR-overexpressed BPH-1siVDR cells was detected by Western blot (top).

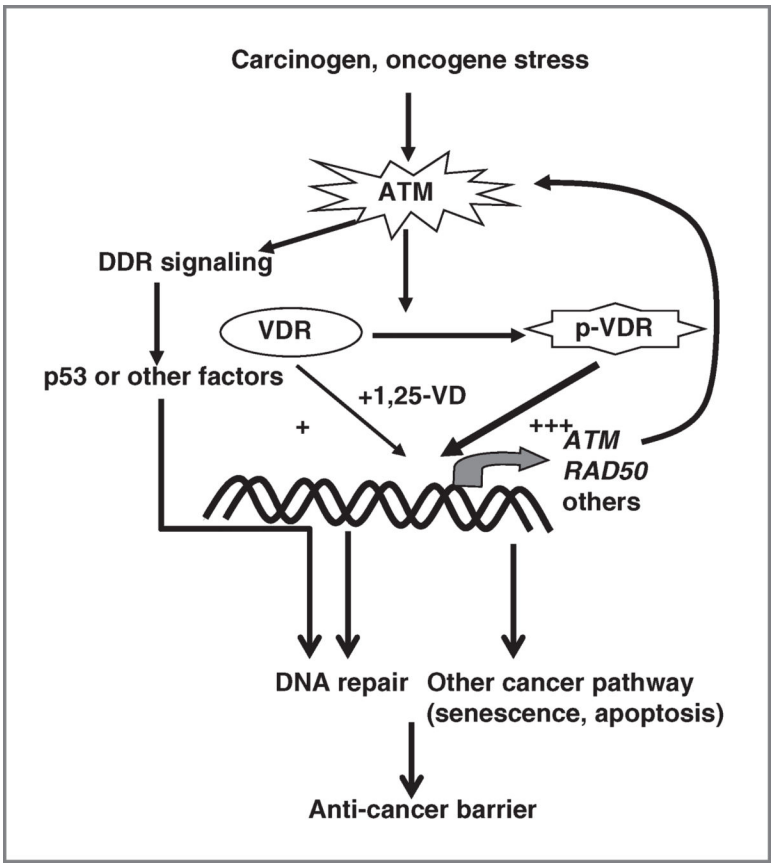

Figure 6.

Schematic diagram of DNA protective and antitumorigenic mechanism of ATM-VDR signaling axis. Carcinogen and other oncogenic stress can stimulate ATM triggering DDR signaling cascade to activate p53 and other factors in forming anticancer barrier in early-stage cancer initiation. Activated ATM can also phosphorylate and enhance VDR transactivity in regulating expression of ATM and RAD50, hence promoting DSB repair guarding genome integrity. Other anticancer pathways, such as senescence and apoptosis, are potentially regulated by 1,25-VD-VDR signaling.